Study of quadratic Zeeman effect in hydrogen at 2-3 MG magnetic fields

V.V. Ivanov[1], R. C. Mancini[1], N. A. Huerta[1], K. J. Swanson[1], D. E. Winget[2], M. H. Montgomery[2], I. E. Golovkin[3], H. K. Hariharan[1], Z. S. Berbel[2]

[1]Department of Physics, University of Nevada, Reno, NV 89557, USA
[2]Department of Astronomy, University of Texas, Austin, TX 78712, USA
[3]Prism Computational Sciences, Madison, WI 53711, USA

The Zeeman effect is used for measurement of magnetic fields in astrophysical and laboratory plasmas. Magnetic fields in atmospheres of magnetic White Dwarf stars are in the range from 40 kG to 1 GG. The quadratic Zeeman effect results in the additional split and shift of lines for magnetic fields > 2 MG. Hydrogen Balmer lines were studied in magnetic fields delivered by a 1 MA pulse power generator. The magnetic field was generated by rod loads 0.8-1 mm in diameter. A droplet of CH oil on the load center was a source of hydrogen. A low ionized oil layer was backlit by black body emission from the rod with a temperature of 0.5-0.6 eV. Zeeman splitting of H-alpha and H-beta absorption lines was studied at magnetic fields with a grating spectrometer. A spectral shift of the central component of the triplet indicated the quadratic Zeeman effect in hydrogen lines. For the first time the quadratic Zeeman effects have been studied in a laboratory setting for hydrogen at 2-3 MG magnetic fields.

I. Introduction

Plasma in strong magnetic fields is the object for research in many fields of basic and applied plasma physics as well as astrophysics. Magnetic fields confine fusion plasma in Tokamaks and can improve conditions for inertial confinement fusion [1]. Heat trapping due to a strong magnetic field plays a key role in the magnetized liner inertial fusion concept [2]. Magnetic fields significantly change the dynamics of plasma expansion and formation of plasma jets and discs [3-6]. Furthermore, laboratory magnetized plasmas can be scaled to plasmas in astrophysical objects [4,7].

For a long time, Zeeman effect was the main spectroscopic feature of plasma in a magnetic field. The Zeeman effect was used for measurements of magnetic fields in Z-pinches and liners. Zeeman splitting of emission lines in Na indicated a 2 MG field in liners on the Z machine [8]. Zeeman effect in indium emission lines was observed at the 5 MG field during the compression of the magnetic flux [9]. The quadratic Zeeman effect appears in hydrogen lines at strong magnetic fields, $B > 2$ MG. The quadratic effect results in the additional fine splitting and spectral shift of Zeeman π and σ components of $H\alpha$ and $H\beta$ triplets [10,11]. Further modelling extended a region of magnetic fields for the Zeeman effect to 1 GG [12], but laboratory plasma experiments were limited by the linear Zeeman effect.

The Zeeman effect has been used to identify magnetic fields in stars via spectroscopy since the beginning of the 20th century [13]. Stellar objects vary widely in magnetic field strength, from the kilogauss level in solar plasma to the gigagauss level in magnetars. White dwarf stars (WD) are of particular interest since they are the evolutionary endpoint of > 97% of all stars, and they often have measurable magnetic fields: Liebert et al. [14] found that at least 10% of WDs have strong magnetic fields over 2 MG, and Ferrario et al. [15] found that of the isolated WDs, 13 ± 4% fall into this high-field regime with magnetic fields from 0.1 MG to 1 GG. In addition, Bagnulo & Landstreet [16] found that the overall incidence of these magnetic WDs is even higher, with 20-

25% of all WDs containing fields from 40 kG to 300 MG. Finally, 36% of cataclysmic variable systems (systems in which a WD accretes material from a main sequence binary companion star) contain a magnetic WD with MG fields [17].

WDs with magnetic fields are observed to have systematically higher masses than their non-magnetic counterparts [18]. This and other evidence suggest that magnetic WDs may be formed through the merger of a WD and another star, with the system passing through a common envelope and/or accretion disk phase. This would naturally account for both their higher masses compared to non-magnetic WDs as well as their observed MG magnetic fields, though this may not be the only mechanism by which strong magnetic fields can form [17,19].

The masses of magnetic WDs are determined by fitting their spectral lines, and these lines are themselves altered by the presence of a magnetic field. Since ~80% of WDs have hydrogen atmospheres, fits to the Balmer series are used to obtain the temperatures and masses of these stars [20]. Models employed in the fits have been developed from a best theory effort. In order to obtain more reliable temperature and mass determinations from spectroscopic fits, the theoretical treatment of these lines in magnetized dense plasmas needs to be tested and validated. The latter necessitates benchmark laboratory experiments with hydrogen at MG-level magnetic fields where experimentally obtained hydrogen absorption lines can be compared with theory calculations of the absorption lines in the atmospheres of magnetic WDs.

In this paper, we investigated, for the first time, the linear and quadratic Zeeman effects in hydrogen at magnetic fields of 2-3 MG in a laboratory setting. The Zeeman split was studied in hydrogen Balmer absorption lines in magnetic fields generated by rod loads. A spectral shift measured for the central π-component due to the quadratic Zeeman effect was in agreement with theory predictions.

II. Experimental setup

A 1 MA Zebra pulsed power generator at the University of Nevada, Reno was used for experiments. A Zebra machine generates a current pulse with a 1 MA amplitude and 80 ns rising edge (10-90%). The Zebra machine can produce strong longitudinal and transverse magnetic fields in coil and rod loads [21]. The magnetic field reaches values of 2-4 MG on the surface of the metal rod loads 0.8-1 mm in diameter. A thin plasma layer arises on the surface at the 30-90% level of the maximum current depending on the rod diameter and material [22]. This surface plasma is confined by the strong magnetic field and slowly expands with a velocity of ~3 km/s. The Doppler spectral shift <0.1 Å is negligible for our experiments. The magnetic field from the load is characterized using Faraday rotation diagnostics and B-dot sensors [23].

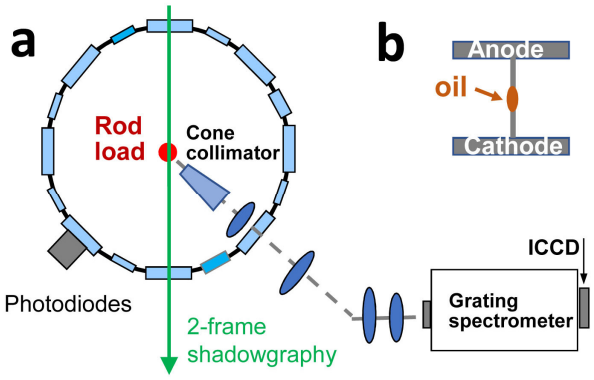

Figure 1. (a) A vacuum chamber, beampath, and grating spectrometer. (b) A rod load between anode and cathode electrodes.

The black body temperature of the surface of the rod load during the current pulse is 0.4-3 eV. The temperature depends on the rod diameter, material, and a value of current. Photodiodes filtered by narrowband interference filters at three

wavelengths are used to monitor the temperature of the load surface. A droplet of CH oil on the load is used as a source of hydrogen. A thin layer of oil is evaporated and heated at the load surface. The external oil layer stays in a liquid and transparent state during the current pulse. Black body emission from the load backlights hydrogen atoms in the evaporated layer. Balmer absorption lines are seen on the black body spectra of loads.

Figure 1 (a) schematically shows a Zebra vacuum chamber with a load, an optical beampath, and a grating spectrometer with two gratings, 1200 l/mm and 2400 l/mm. The rod load, 2 cm tall is installed in the center of the chamber. A cone collimator selects emission only from the center of the load covered with oil, and a four-lens optical beampath relays emission from the load center to the 50 μm slit of the spectrometer. The rod load between anode and cathode with the oil droplet is shown in Fig. 1 (b).

Intensified charge coupled device (ICCD) camera with a matrix of 1K x 1K pixels and microchannel plate (MCP) was used as a sensor of the grating spectrometer. A 3-6 ns gate of MCP provided temporal resolution of spectral measurements on the 80 ns rising edge of current. Dispersion of the spectrometer with the ICCD sensor measured at the wavelength of the Hα line was -0.4 Å /px with the 1200 l/mm grating and -0.16 Å/px with the 2400 l/mm grating. Spectral ranges were 400 Å and 160 Å for two gratings, respectively. Neon, xenon, and hydrogen lamps were used for spectral calibration in the ranges near Hα and Hβ lines at wavelengths of 656 nm and 486 nm.

A diameter and material of rod loads were varied to reach the highest magnetic field before the intensive evaporation of the load material. Simulations with a PrismSPECT program [24] showed that the optimal temperature of hydrogen is in the range of 0.5 - 0.6 eV because the line width strongly increases at the temperature > 0.7 eV. Line absorption drops below the noise at the at temperatures < 0.4 eV. Some materials like titanium and stainless steel were not used due to strong absorption lines generated in the range near Hα and Hβ hydrogen lines.

III. Zeeman effect at 2-3 MG magnetic fields

The quadratic Zeeman effect results in the fine splitting and spectral shift of components of Zeeman triplets in magnetic fields >2MG. A theoretical approach to the Zeeman effect in MG magnetic fields was presented in reviews [10,12]. For Balmer transition *2S – nP*, the center of mass of the line averaged over π and σ components is shifted to short wavelengths due to the quadratic Zeeman effect [12]:

$$\delta\lambda_Q(2S) = -1.73\left(\frac{\lambda}{4101A}\right)^2\left(\frac{B}{10^6G}\right)^2\left(\frac{n_{up}}{6}\right)^4 A$$

where λ is a wavelength, B is the magnetic field, and n_{up} is the upper principal quantum number. The shifts are smaller ~ 40% for *2P- nS* and *2P- nD* transitions. A detailed table of the quadratic splitting with quantum numbers for transitions is presented in [10].

A series of shots was performed to confirm a capability of experimental methods and diagnostics for observation of the Zeeman effect in MG magnetic fields. Aluminum rod loads, 1 mm in diameter provided conditions suitable for observation of Hα line for current up to 0.8 MA. Polarization and intensity of Zeeman components depend on the direction to the vector of the magnetic field [25]. σ components are too wide and weak if a circular cross section load with the azimuthal magnetic field was used. A flat center of the load was employed to enhance a visibility

of σ components of the Zeeman triplet. The magnetic field was enhanced along the sight of view. This configuration also decreased spanning in a large range of field strengths in cylindrical loads.

Figure 2 (a) presents absorption Zeeman spectra from four shots with Al loads at current of 0.78 MA. Spectra fade at higher current due to the fast evaporation of the load material. Spectra in Fig. 2 are recorded with the 1200 l/mm grating calibrated with spectral lamps. Color lines show spectra from several shots. Averaging of shots is shown in black and clearly shows a central π component near 656 nm and two wide σ "wings" of the Hα Zeeman triplet. "Wings" are wide compared to the central part due to strengths of components of the B-field may vary on the load. Zeeman σ components are shifted on 3.8-3.9 nm from the π component to the centers of "wings". The magnetic field B can be calculated from the spectral split using a Paschen - Back formula $E = E_0 \pm \mu_B B$, where μ_B is the Bohr magneton and E is the energy level. The magnetic field is B=1.9 ± 0.1 MG. An additional quadratic shift of σ components is 0.07 nm at the 2 MG magnetic field [11]. Values of magnetic fields taken from the Zeeman splitting agree with measurements of the magnetic field by Faraday rotation and B-dot diagnostics with uncertainty of 5-8%. A shift and width of σ components are measured with an error due to small absorption and shot-to-shot variation of the machine. σ components were not used for further precision measurements. We note that the value of the split represents a value of the local magnetic field seen by hydrogen atoms compared to the integrated magnetic fields taken at the distance from the load with Faraday and B-dot diagnostics.

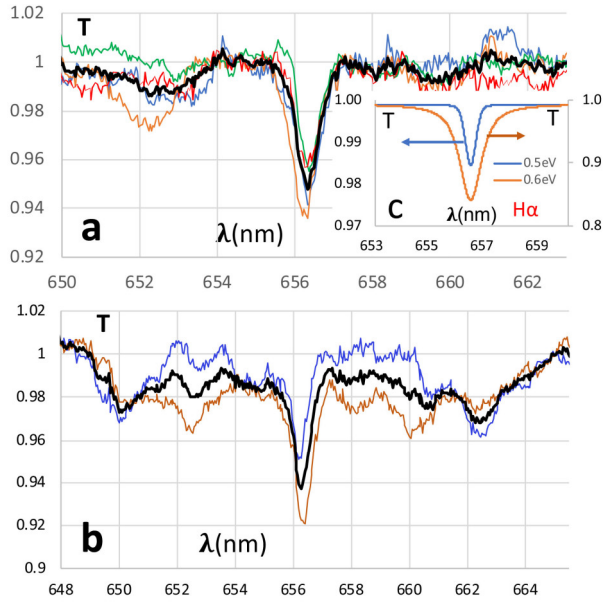

Figure 2. (a) Hα Zeeman triplets from four shots with Al loads 1mm in diameter. (b) Zeeman triplets from two shots with Cu loads 0.9 mm in diameter. (c) PrismSPECT simulations of transmission of the Hα line at 0.5 eV and 0.6 eV.

Figure 2 (b) shows Hα spectra taken from two shots with Cu loads 0.9 mm in diameter. These loads allow measurements of Zeeman effect near the maximum of the current pulse. The Zeeman split ~6.2 nm in Fig. 2 (b) corresponds to the local magnetic field of ~3 MG.

Absorption of the central line in Fig. 2 is 5-7 % and a line width is 0.5-0.7 nm. These parameters of the absorption line are in agreement with PrismSPECT simulations for hydrogen without magnetic fields with an electron temperature of 0.5 - 0.6 eV, density of 10 mg/cm^3, and width of the layer of 0.3 mm as shown in Fig. 2 (c). The line broadens at higher densities. Hβ Zeeman triplets were also observed with Al loads but with weaker absorption. Uncertainties of measurements in Fig. 2 do not allow identification of the quadratic Zeeman effect. Wide σ components with small intensities cannot be used for precision measurements. Apparatus and procedures were improved for investigation of the quadratic effect as shown in the next section.

IV. Quadratic Zeeman effect

Atomic simulations for a hydrogen atom in strong magnetic fields showed that the quadratic Zeeman effect produces an additional fine splitting of lines of the Zeeman triplet and spectral shifts of the π and σ components of Hα and Hβ triplets [10,11]. Fine structure of the additional split cannot be resolved in our case. These splitting results in a broadening of the central π line and σ components. σ components are wide and their absorption is low. A width of the central component includes contributions of temperature and instrumental broadenings. The most promising method to identify the quadratic effect is measuring the spectral shift of the central π line to the shorter wavelength. The spectral shift of the center of mass for hydrogen Hα and Hβ Zeeman lines in the magnetic field of 1-5 MG was calculated by [11]. For example, the shift of the Hα central line is expected to be 0.36 Å at B=2 MG. The spectral shift is higher for the Hβ transition at the wavelength of 486 nm, 0.97 Å at the same B=2 MG. The Hβ line has a weaker absorption compared to the Hα line due to the smaller oscillator strength for this transition.

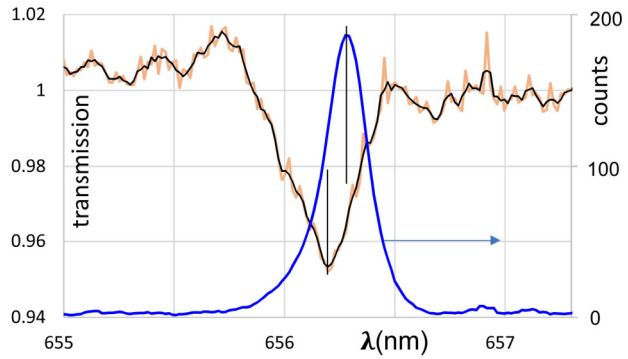

Figure 3. A blue line is a Hα emission reference line from the hydrogen lamp. A red line is an absorption line from hydrogen in the magnetic field of the rod load with an average black line.

Apparatus and procedures were improved to provide higher accuracy and reproducibility of spectral measurements. The spectrometer and ICCD camera were protected against shocks and vibration during operations. A 2400 l/mm grating was used for investigation of the quadratic Zeeman effect. The spectral shift of the minimum of Hα or Hβ absorption lines in the magnetic field was compared to the peak of reference Hα or Hβ emission lines taken from the hydrogen spectral lamp as shown in Fig. 3. Reference Hα and Hβ lines were recorded right before every shot with the load and magnetic field. A width of reference hydrogen lines was 12-14 pixels, but peaks of lines were reproducible with accuracy of 0.5 pixels. The optical beampath was tested with a hydrogen lamp installed in the vacuum chamber on the load position. Accuracy of measurement of the spectral shift was better than 1 pixel of the ICCD camera.

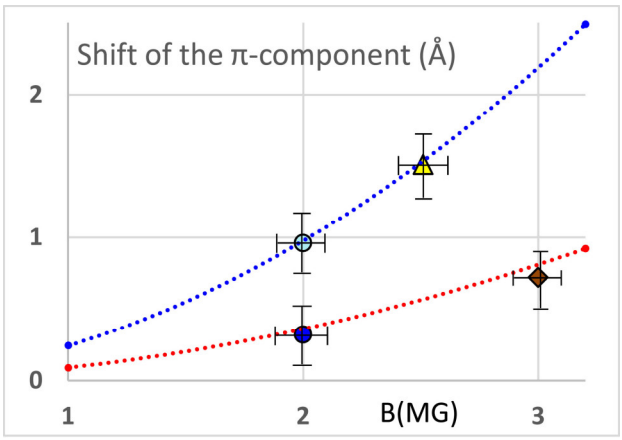

Figure 4. Dotted lines present calculations of Surmelian & O'Connell (1974) of the spectral shift of Hα (red line) and Hβ (blue line) central component due to the quadratic Zeeman effect. Experimental points are taken with Al 1 mm loads (circles), Au 1 mm loads (triangle), and Cu 0.9 mm loads (diamond).

We used Al 99.9% rod loads, 1 mm in diameter at current 0.78 MA when the magnetic field was 1.9 MG. Cu 99.99% rod loads, 0.9 mm in diameter allowed generation of 3 MG fields near the maximum of the currant pulse. Copper loads were used for Hα line at the wavelength of 6562.8 Å but not used for the Hβ line because of Cu spectral lines generated near

4862 Å. Au 99.99% rod loads 1 mm in diameter provided 2.5 MG magnetic fields. Au loads generate a strong line at 6562.8 Å but can still be used in the range near the Hβ line. Figure 3 and Figure 4 show results of experiments with these loads. A wavelength of the absorption peak was measured as seen in Fig. 3. The experimental points in Fig. 4 are the laboratory measurements of the quadratic Zeeman effect in hydrogen Hα and Hβ lines for magnetic fields of 2-3 MG. Experimental points are placed on dotted lines taken from calculations of [11] for the quadratic Zeeman shift. The dotted lines interpolate calculations for Hα and Hβ lines at 1, 2, 3.2, and 5 MG. A diamond marker presents an average value for 3 shots with Cu loads 0.9 mm in diameter. A triangle shows the average for 2 shots with 1 mm Au loads. Circles present shots with 1 mm Al loads. A filled circle presents one shot at the Hα wavelength. An open circle presents the average of two shots at the Hβ wavelength. Variations of magnetic fields are due to the shot to shot reproducibility of the current pulse on the load. Experimental points are in agreement with interpolated lines.

V. Conclusions

The quadratic Zeeman effect in hydrogen at magnetic fields of 2-3 MG was studied in a laboratory. An experimental platform based on the 1 MA pulsed power machine allowed for investigation of plasmas at 1-3 MG magnetic fields. A layer of oil on the rod load was employed as a source of hydrogen. Rod loads generated MG magnetic fields, populated the second level of hydrogen, and backlit hydrogen atoms. We optimized load materials, load diameters, and current in the load and found a regime appropriate for the observation of hydrogen Balmer absorption lines.

Absorption in hydrogen Hα central π line is 3-5%. A spectral shift of σ components in the Hα Zeeman triplet indicates magnetic fields in the range of 2-3 MG in Al, Au, and Cu loads. These values are in agreement with other diagnostics. A width of the central π component of the Hα Zeeman triplet is 0.5-0.7 nm. The absorption π line was used for measuring the spectral shift of the line peak due to the quadratic Zeeman effect. The spectral shift of Hα and Hβ absorption lines in magnetic fields was measured compared to the reference Hα and Hβ emission lines from the hydrogen spectral lamp. The experimental spectral shifts are in agreement with calculations of the quadratic Zeeman effect for these hydrogen lines in this range of magnetic fields.

The influence of the quadratic Zeeman effect in the range of 2-3 MG fields can be found in hydrogen spectra of atmospheres of magnetic White Dwarf stars if measured and analyzed with high spectral resolution. We note that carbon absorption lines are seen in atmospheres of some magnetic White Dwarf stars [26]. Carbon lines can be investigated in the laboratory with the same technique in future experiments.

Acknowledgements

The authors thank the team of the Zebra generator at UNR for help with experiments. This work was supported by the DOE NNSA under the award DE-NA0003991, and partly by the NSF award PHY-1903355 through the NSF-DOE Partnership in Basic Plasma Science and Engineering. D.E.W., M.H.M., and Z.S.B. acknowledge support from the Wootton Center for Astrophysical Plasma Properties under U.S. Department of Energy cooperative agreement number DE-NA0003843, and the National Science Foundation under grant AST 1707419.

1. P. Y. Chang, G. Fiksel, M. Hohenberger, J. P. Knauer, R. Betti, F. J. Marshall, D. D. Meyerhofer, F. H. Séguin, and R. D. Petrasso, *Phys. Rev. Letts.,* **107**, 035006 (2011).
2. S. A. Slutz, R. A. Vesey, *Phys. Rev. Lett.* **108**, 025003 (2012).
3. V. V. Ivanov, A.V. Maximov, R. Betti, P.P. Wiewior, P. Hakel, M. E. Sherrill, *Plasma Phys. Control. Fusion* **59**, 085008 (2017).
4. B. Albertazzi, A. Ciardi, M. Nakatsutsumi, T. Vinci, J. Béard, R. Bonito, J. Billette, M. Borghesi, Z. Burkley, S. N. Chen et al., *Science,* **346,** 325 (2014).
5. R. Presura, V. V. Ivanov, Y. Sentoku, V. I. Sotnikov, P. J. Laca, N. Le, Galloudec, A. Kemp, R. Mancini, H. Ruhl, A.L. Astanovitskiy et al., *Astrophysics and Space Science* **298,** 299 (2005).
6. V. V. Ivanov, A. V. Maximov, R. Betti, L. Leal, R. C. Mancini, K. J. Swanson, I. Golovkin, C. J. Fontes, H. Sawada, A. B. Sefkow et al., *Phys. Plasmas* **26**, 062707 (2019).
7. R. E. Falcon, G. A. Rochau, J. E. Bailey, T. A. Gomez, M. H. Montgomery, D. E. Winget, T. Nagayama, *ApJ*, **805**, 214 (2015).
8. M. R. Gomez, S. B. Hansen, K. J. Peterson, D. E. Bliss, A. L. Carlson, D. C. Lamppa, D. G. Schroen, G. A. Rochau, Rev. Sci. Instrum. **85**, 11E609 (2014).
9. W. B. Garn, R. S. Caird, D. B. Thomson, C. M. Fowler, , Rev. Sci. Instrum., **37**, 762 (1966).
10. R. H. Garstang, Rep. Prog. Phys., **40**, 106 (1977).
11. G. L. Surmelian, R. F. O'Connell, ApJ **193**, 705 (1974).
12. D. T. Wickramasinghe, L. Ferrario, The Astronomical Society of the Pacific, **112**, 873 (2000).
13. G. E. Hale, ApJ **28**, 315 (1908).
14. J. Liebert, P. Bergeron, J. B. Holberg, ApJ **125**, 348 (2003).
15. L. Ferrario, D. T. Wickramasinghe, A. Kawka, Advances in Space Research **66**, 1025 (2020).
16. S. Bagnulo, J.D. Landstreet, MNRAS **507**, 5902 (2021).
17. A. F. Pala, B. T. Gänsicke, E. Breedt, C. Knigge, J. J. Hermes, N. P. Gentile Fusillo, M. A. Hollands, T. Naylor, I. Pelisoli, M. R. Schreiber et al., MNRAS **494**, 3799 (2020).
18. J. McCleery, P. E. Tremblay, N. P. G. Fusillo, M. A. Hollands, B. T. Gänsicke, P. Izquierdo, S. Toonen, T. Cunningham, A. Rebassa-Mansergas, MNRAS **499**, 1890 (2020).
19. D. Stello, M. Cantiello, J. Fuller, D. Huber, R. A. García, T. R. Bedding, L. Bildsten, V. S. Aguirre, Nature **529**, 364 (2016).
20. A. Raji, J. Rosato, R. Stamm, Y. Marandet, Eur. Phys. J. D **75**, 63 (2021).
21. V. V. Ivanov, A. V. Maximov, R. Betti, L. S. Leal, J. D. Moody, K. J. Swanson, N. A. Huerta, Matter and Radiation in Extremes **6**, 046901 (2021).
22. K. C. Yates, B. S. Bauer, S. Fuelling, T. J. Awe, T. M. Hutchinson, V. V. Ivanov, J. Mei, R. S. Bauer, Phys. Plasmas **26**, 042708 (2019).
23. V. V. Ivanov, K. J. Swanson, G. S. Sarkisov, A. V. Maximov, P. Wiewior, A. Astanovitskiy, V. Nalajala, O. Chalyy, O. Dmitriev, N. Wong, Phys. Plasmas **24**, 112707 (2017).
24. J. J. MacFarlane, I. E. Golovkin, P. Wang, P. R. Woodruff, N. A. Pereyra, HEDP **3**, 181 (2007).
25. E. Landi Degl'Innocenti, M. Landolfi, "*Polarization in Spectral Lines",* Astrophysics and Space Science Library **307**; Dordrecht: Kluwer (2004).
26. K. A. Williams, D. E. Winget, M. H. Montgomery, P. Dufour, S. O. Kepler, J. J. Hermes, R. E. Falcon, K. I. Winget, M. Bolte, K. H. R. Rubin et al., ApJ, **769**, 123 (2013).